ISSN 1027-5495. Functional Materials, 30, No.1 (2023), p. 12-17.
doi:https://doi.org/10.15407/fm30.01.12

1. Physical parameters of the energy barrier of graphene/p–CdTe Schottky diodes

***I.P.Koziarskyi*[1], *M.I.Ilashchuk*[1], *I.G.Orletskyi*[1], *L.A.Myroniuk*[1,2], *D.V.Myroniuk*[1,2], *E.V.Maistruk*[1], *D.P.Koziarskyi*[1], *I.M.Danylenko*[3]**

[1]Yuriy Fedkovych Chernivtsi National University, 2 Kotsyubynskyi Str.,
58002 Chernivtsi, Ukraine
[2]I.M.Frantsevich Institute for Problems of Materials Science, National
Academy of Sciences of Ukraine, 60 Nauky Ave., 3 Krzhyzhanovsky Str.,
03142 Kyiv, Ukraine
[3]V.Lashkaryov Institute of Semiconductor Physics, National Academy of
Sciences of Ukraine, 45 Nauky Ave., 03028 Kyiv, Ukraine

Received October 20, 2022

Graphene/p–CdTe Schottky diodes were obtained by spaying polyvinylpyrrolidone solutions of particles of multilayer graphene. It was established that the spray process does not affect the electrical parameters of the substrates when they are heated to a temperature of $T_S = 523$ K. The formation of graphene layers was confirmed by the study of Raman scattering spectra in the frequency range of 1000–3250 cm^{-1}, which correspond to the vibrations of carbon sp^2 bonds. The intense peak of the 2D band and its asymmetry indicate the presence of graphene on p–CdTe substrates and its multilayer nature. Based on the study of the temperature dependence of the I–V-characteristics, the diode properties of the investigated graphene/p–CdTe structures were established, the energy barrier height $q\varphi_k = 0.75$ eV and the temperature coefficient of its change $d(q\varphi_k)/dT = -2.6 \cdot 10^{-3}$ eV/K were estimated. The temperature dependence of the series resistance of the structure was analyzed and the ionization energy of the energy level responsible for the equilibrium conductivity in the base material was determined. The analysis of the C–V-characteristics measured in a wide frequency range from 10 kHz to 1000 kHz made it possible to determine the main physical parameters of the energy barrier, as well as the impurity concentration and its distribution in the p–CdTe region. It was confirmed that the concentration of the electrically active acceptor impurity in the near-contact region of the p–CdTe substrate coincides with the concentration of holes in the base material.

Keywords: graphene, Schottky diodes, CdTe, energy barrier.

Фізичні параметри енергетичного бар'єру діодів Шотткі графен/p–CdTe. *І.П.Козярський, М.І.Ілащук, І.Г.Орлецький, Л.А.Миронюк, Д.В.Миронюк, Е.В.Майструк, Д.П.Козярський, І.М.Даниленко*

Діоди Шотткі графен/p–CdTe були отримані розпиленням полівінілпіролідонових розчинів із частинками багатошарового графену. Встановлено, що процес напилення не впливає на електричні параметри підкладок при їх нагріванні до температури $T_S = 523$ К. Утворення графенових шарів підтверджено дослідженнями спектрів комбінаційного розсіяння в діапазоні частот 1000–3250 cm^{-1}, що відповідає коливанням вуглецевих sp^2-зв'язків. Інтенсивний пік 2D смуги та її асиметрія вказують на наявність графену на підкладках p–CdTe та його багатошаровість. На основі дослідження температурних залежностей I–V-характеристик встановлено діодні властивості досліджуваних структур графен/p–CdTe, проведена оцінка висоти енергетичного бар'єру $q\varphi_{ik} = 0.75$ eV та температурного коефіцієнта її зміни I$d(q\varphi_k)/dT = -2.6\cdot10^{-3}$ eV/K. Проаналізована температурна залежність послідовного опору структури та визначена енергія іонізації енергетичного рівня, що відповідає за рівноважну провідність у базовому матеріалі. Аналіз вольт-фарадних характеристик, виміряних у широкому діапазоні частот від 10 kHz до 1000 kHz, дав можливість визначити основні фізичні параметри енергетичного бар'єру, а також концентрацію домішки та її розподіл в області p–CdTe. Підтверджено, що концентрація електроактивної акцепторної домішки в приконтактній області підкладки p–CdTe збігається з концентрацією дірок в основному матеріалі.

1. Introduction

Graphene is a two-dimensional crystal whose multifaceted chemical and physical properties are determined by its crystal structure and π-electron system. Today, this is an object of scientific research and practical use [1–8]. Graphene is a material characterized by many unique properties: high mobility of charge carriers (~ $1\text{–}1.5\cdot10^4$ $\mathrm{cm^2\cdot V^{-1}\cdot s^{-1}}$ for graphene on a SiO_2/Si substrate and up to $2.0\cdot10^5$ $\mathrm{cm^2\cdot V^{-1}\cdot s^{-1}}$ for suspended graphene [8]), high conductivity (550 S/cm [9]), significant transparency in the visible, ultraviolet (83.7–97.1 % [10]) and near infrared (70 % [9]) spectral regions, record mechanical strength (Young's modulus ~ 1 TPa [8]), chemical and thermal (graphene melting temperature about 5000 K [11]) stability. Due to the modulated value of the thermodynamic work function of electrons [11] and the possibility of changing the position of the Fermi level relative to the Dirac points, the specified electrical and optical properties of graphene make it possible to use thin films of graphene in Schottky diodes with rectifying properties [8]. Such surface-barrier structures have practical application in high-performance and inexpensive IR photodetectors, solar cells, which have already reached an efficiency of ~ 15 % [8]. Transparent, conductive, and ultrathin graphene films are an excellent alternative to commonly used metal oxide window electrodes for solar cells based on currently known absorbers (Si, CdTe, $CuInGaSe_2$(CIGS), perovskite [8, 10, 11, 12]). Heterostructures based on p–CdTe, in which the frontal contact was formed as graphene/ZnO, showed a photovoltaic conversion efficiency of 4.17 % [10]. The use of graphene doped with boron for the manufacture of the back contact allowed the authors to increase the efficiency of these photoconverters to 9.1 % [11]. In addition, the created solar cells have a relatively large active area (1.0 $\mathrm{cm^2}$), which indicates the possibility of manufacturing large-scale devices. An increase in the efficiency of graphene/p–CdTe Schottky diodes from the initial 2.08 % to 3.10 % was observed when CdSe quantum dots were deposited on the graphene front contact surface [13]. An increase in the efficiency of CdS/CdTe solar cells up to 12.1 % (which is higher compared to traditional back contacts based on graphite doped with copper particles (10.5 %) or thin copper films (9.1 %)) was achieved using Cu-nanowire-doped graphene (Cu NWs/graphene) [14].

In addition to the experimental results presented in the works cited above, theoretical modeling of CdS/CdTe thin-film solar cells with graphene nanolayers used as front and back electrodes was carried out [15]. Simulations show that graphene reduces reflection and absorption losses and increases the value of the short circuit current J_{sc} compared to TCO (Transparent Conductive Oxide). The authors optimized the number of graphene layers and showed that single-layer graphene has lower optical losses. The graphene back-contact structure has another advantage, as it allows two-way irradiation. The J_{sc} value of this structure increased from 25 $\mathrm{mA/cm^2}$ to almost 40 $\mathrm{mA/cm^2}$. Another promising practical application of graphene/p–CdTe Schottky diodes are γ- and X-ray detectors, which have shown promising spectral resolution of ^{241}Am (59 keV) and ^{137}Cs (662 keV) isotopic radiation at room temperature[16].

It should be noted that, in the cited works, graphene thin films were obtained by chemical vapor deposition (CVD), which is currently the main method both in scientific circles and in industry [12]. Despite the fact that the graphene films obtained by this method are of high quality and have a rather large area [12], the technological process of their production is quite complicated and energy-consuming, since it takes place at a high temperature ($T \approx 1000$°C). Since the mechanical exfoliation of graphite to graphene is a simple and inexpensive method, it has been proposed to obtain sufficiently high-quality graphene layers by dispersing and exfoliating graphite in organic solvents such as N-methylpyrrolidone using sonication [17] or a kitchen blender

[18]. However, the use of methylpyrrolidone is environmentally dangerous due to its high toxicity [17, 18]. Therefore, methylpyrrolidone is often replaced by non-toxic polyvinylpyrrolidone (PVP) [19, 20].

The main task of the work was to obtain graphene/p–CdTe Schottky diodes by applying multilayer graphene obtained by the method of mechanical exfoliation of graphite in an aqueous solution of polyvinylpyrrolidone (PVP), and to determine the physical parameters of the energy barrier.

2. Experimental

The substrates used for the manufacture of graphene/p–CdTe Schottky diodes were obtained by cleavage from crystalline ingots of unalloyed cadmium telluride, grown by the vertical Bridgman method under low pressure of cadmium vapors in an ampoule. The crystals have hole conductivity. Their specific electrical conductivity was $\sigma = 3\cdot10^{-3}\ \Omega^{-1}\cdot\text{cm}^{-1}$ at $T = 301$ K, and the concentration and mobility of holes, respectively, $p = 3.5\cdot10^{14}\ \text{cm}^{-3}$ and $\mu_H = 56.0\ \text{cm}^2\cdot\text{V}^{-1}\cdot\text{s}^{-1}$. The dominant point defects that form in CdTe crystals under these growth conditions are singly charged cadmium vacancies V^{-}_{Cd} or complexes with their participation, which are acceptor defects and cause hole conductivity of the material [21]. The predominant concentration of vacancies in the Cd lattice is explained by the ratio of the partial pressures of the Cd and Te components ($P_{\text{Cd}} = 2P_{\text{Te2}}$) [21]. To obtain graphene layers on the surface of the substrate, the method of mechanical exfoliation of graphite in organic solvents using a kitchen blender was used. Powdered casting graphite (GL-1) and an aqueous solution of polyvinylpyrrolidone (PVP) $(C_6H_9NO)_n$ were used to form a dispersed mixture. Graphite crystals were dispersed in PVP with a concentration of 3 mg/ml to form 500 ml of graphite dispersion (15 mg/ml). The exfoliation process of graphite to graphene took place under the mechanical action of the blender, the speed of which was 8500–9000 rpm. Further separation of the liquid and solid fractions of the mixture was carried out using a centrifuge. The resulting precipitate was diluted with ethyl alcohol and applied to the cleaned substrates using a pneumatic atomizer. The complete removal of volatile components of the solution from the deposited films occurred at a substrate temperature not higher than $T_S = 523$ K. This ensured the stability of the electrical parameters of the base material in the process of manufacturing the structures. The formation of graphene layers was confirmed by Raman scattering spectra recorded on a Jobin Yvon t64000 Raman spectrometer upon excitation with unpolarized light with a wavelength of 514.5 nm.

Ohmic contacts to p–CdTe substrates [22] were obtained by creating a p^+-region in the near-surface layer. To do this, their surface was pretreated with a ruby laser (wavelength $\lambda = 0.694$ μm, photon energy $h\nu = 1.79$ eV). High-power laser radiation with photon energy greater than the CdTe band gap ($h\nu > E_g = 1.5$ eV) leads to melting, recrystallization, and evaporation of surface components. At the same time, the surface is enriched with its own point defects of the acceptor type, cadmium vacancies (V_{Cd}), which causes the formation of the p^+-region. Next, ohmic contacts were formed by deposition of gold and copper from aqueous solutions of their salts. The contact to the graphene layers was formed using a silver-based conductive paste.

The I–V-characteristics of the investigated graphene/p–CdTe Schottky diodes were measured using a hardware-software complex implemented on the basis of the Arduino platform, an Agilent 34410A digital multimeter and a Siglent SPD3303X programmable power source, which were controlled by a personal computer using software created by the authors in the LabView environment. The measurements of capacitance-voltage (C–V) characteristics of structures in a wide frequency range of the measuring signal were carried out using a LCR Meter BR2876.

3. Results and discussion

The Raman scattering spectrum of the graphene is characterized by one sharp and symmetrical peak of the 2D band. Since graphite consists of several graphene monolayers, the 2D band observed in its spectrum is wider and asymmetric compared to the 2D band in the graphene spectrum [17]. This indicates the presence of several components with several phonon modes, as can be seen from the comparison of the spectra shown in Fig. 1. Some observed asymmetry of the 2D band in the graphene spectrum indicates its multilayered nature.

The I–V-characteristics of graphene/p–CdTe Schottky diodes measured in the temperature range $T = 301$–340 K are shown in Fig. 2. The current rectification ratio in the

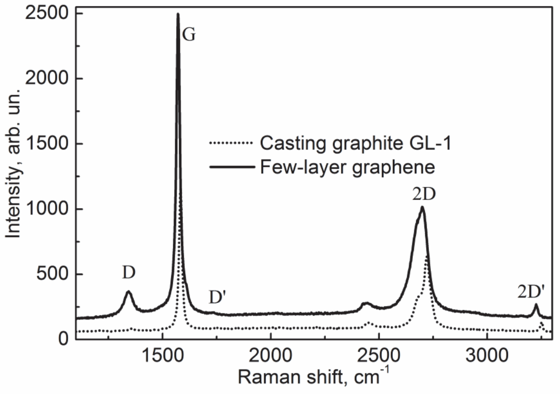

Fig. 1. Raman spectra of casting graphite and few-layer graphene (FLG).

manufactured structures was ~ 10^2 at T = 301 K and voltage $|V| = 1$ V. The voltage value φ_k, at which there is a significant increase in forward current, can be interpreted in the first approximation as the value of the built-in potential; it was estimated by extrapolation of the linear sections of the I–V-characteristics with a forward bias on the voltage axis (at T = 301 K, the value of φ_k = 0.75 V).

The temperature coefficient of its change was determined from the temperature dependence of the height of the potential barrier $q\varphi_k$; it was $d(q\varphi_k)/dT = -2.6\cdot10^{-3}$ eV/K (Fig. 2, inset a), which correlates well with the results obtained for barrier structures based on CdTe and solid solutions based on it $Cd_{-x}Zn_xTe$ [23, 24].

Taking into account the geometric dimensions of the substrate, the series resistance ($R_S \approx 1.4\cdot10^2$ Ω) of the structure correlates well with the resistance of the CdTe base material. The practically absent temperature dependence of R_S is explained by the presence of the depletion region of the shallow acceptor level E_V+0.05 eV in the temperature range of measurements. This determines the equilibrium conductivity of low-impedance undoped p–CdTe obtained under the specified technological conditions [21]. It is known that this energy level corresponds to a singly charged vacancy of cadmium V_{Cd}^{-1}, or a complex with its participation [21].

The C–V-characteristics of graphene/p–CdTe Schottky diodes in the frequency range f = 10–100 kHz (Fig. 3) and f = 200–1000 kHz (Fig. 4) show the dynamics of changes in the thickness of the space charge region, which is depleted by the main charge carriers (holes) from the side of p–CdTe at reverse voltages and an increase in the conductivity of the structure at forward biases. At low frequencies f = 10–20 kHz, with reverse biases -0.5 V < V < 0 V, a lower rate of change in capacitance with voltage is observed, which is related to the contribution of the capacitance of the energy states at the edge of the electrical transition to the total capacitance of the structure. At forward voltages 0 < V < 0.4 V, the capacity of the graphene/p–CdTe diode increases due to the narrowing of the area depleted by the charge carriers. At V > 0.4 V, the measured capacity decreases due to an increase in the conductivity of the structure.

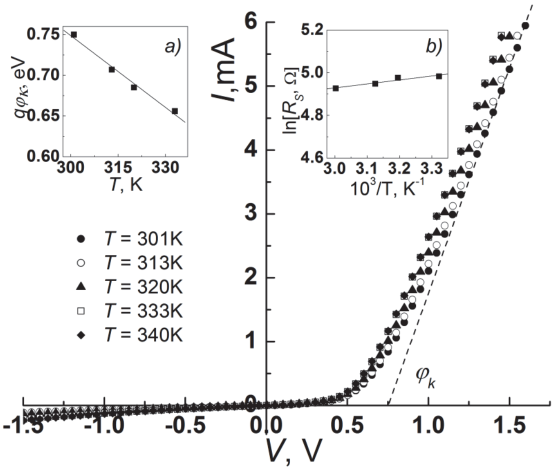

Fig. 2. I–V-characteristics of graphene/p–CdTe Schottky diodes in the temperature range T = 301–340 K. The inset shows temperature dependences of the height of the potential barrier $q\varphi_k$ (a) and series resistance R_S of the structure (b).

To determine the main parameters of the investigated graphene/p–CdTe Schottky diodes, the analysis of C–V-characteristics was carried out at high frequencies in order to avoid the influence of the charge of deep levels on the value of the measured capacitance (Fig. 5).

The capacitance of graphene/p–CdTe Schottky diodes is determined by the charge of the depletion region in p–CdTe in the reverse voltage region. The observed parallel shift of the linear sections of the dependences $1/C^2 = f(V)$ as the frequency changes from 500 kHz to 1000 kHz indicates the influence of the series resistance R_S of the structure on the value of the measured capacitance.

In this case, the total capacity C is described by the expression [25]:

$$C^{-2} = C_0^{-2} + 2\overline{\omega}^2 R_S^2, \qquad (1)$$

where C_0 is the capacitance of the charge region.

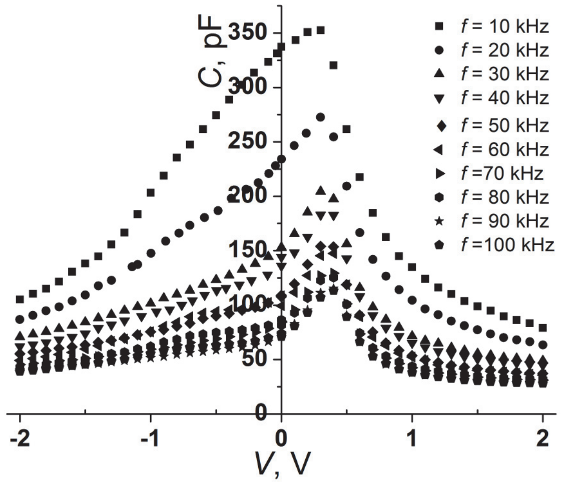

Fig. 3. C–V-characteristics of graphene/p–CdTe Schottky diodes in the low-frequency region (f = 10–100 kHz).

The contact potential difference φ_k was determined by a well-known method, taking into account the frequency dependence of the measured capacitance C according to expression (1) from the plotted dependence $V = f(\overline{\omega}^2)$ (Fig. 5 inset). The V_0 value was obtained by extrapolation of the rectilinear sections of the function $C^{-2} = f(V)$ on the voltage axis. The obtained value φ_k = 0.8 eV is in good agreement with the value determined from the analysis of the forward branches of the I–V-characteristics (φ_k = 0.75 eV).

The concentration of the electrically active acceptor impurity N_A in the charged region of the p–CdTe diode was determined by the expression [26]:

$$\mathrm{tg}\alpha = \frac{2}{q\varepsilon_S\varepsilon_0 N_A S^2}, \tag{2}$$

where q is the electron charge; S is the area of the electrical transition; ε_S = 10.6 is the relative permittivity of CdTe; $\varepsilon_0 = 8.85\cdot10^{-12}$ F/m is the electrical constant. The calculated concentration of acceptors $N_A = 2.2\cdot10^{14}$ cm^{-3} is in good agreement with the concentration of holes in the base material ($p = 3.5\cdot10^{14}$ cm^{-3}), which confirms the stability of the electrical parameters of the base material during the fabrication of structures.

The electrical junction thickness $d \approx 2.8$ μm of the graphene/p–CdTe diodes has been determined from the expression for a flat capacitor

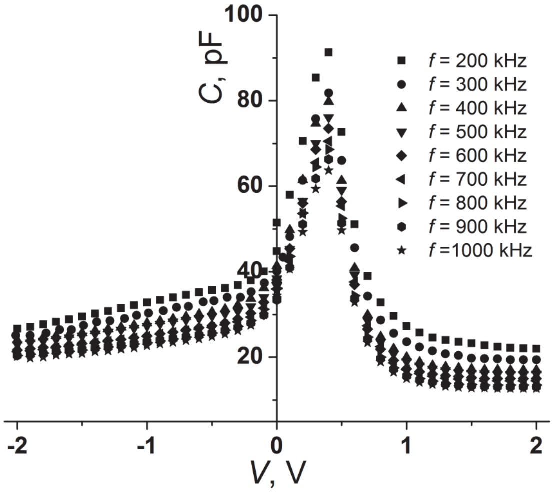

Fig. 4. C–V-characteristics of graphene/p–CdTe Schottky diodes in the high-frequency range (f = 200–1000 kHz).

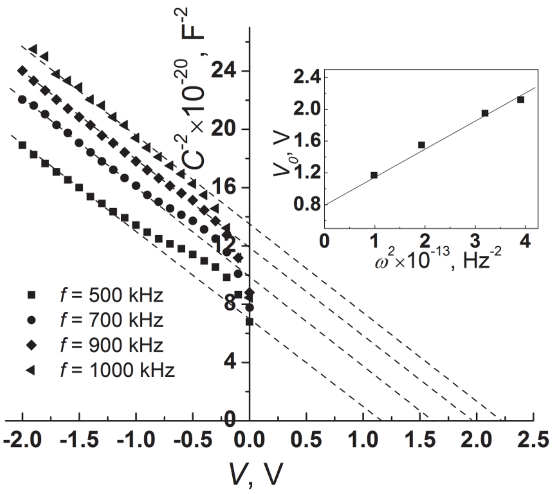

Fig. 5. Dependence $C^{-2} = f(V)$ for graphene/p–CdTe Schottky diodes at frequencies 500 kHz <<|f <<|1000 kHz and dependence $V_0 = f(\overline{\omega}^2)$ (inset).

$$C = \frac{\varepsilon_0\varepsilon_s S}{d}. \tag{3}$$

4. Conclusions

Graphene/p–CdTe Schottky diodes with a current rectification factor ~ 10^2 were obtained by mechanical exfoliation of graphite with the formation of few-layer graphene in a polyvinylpyrrolidone (PVP) aqueous solution. The intense peak of the 2D band in the Raman scattering spectrum and its asymmetry indicate the presence of graphene on the p–CdTe substrate and its multilayer nature. The diode properties of the investigated graphene/p–CdTe structures are due to the energy barrier of 0.8 eV formed in the near-contact region of p–CdTe.

Analysis of the C–V-characteristics indicates that the obtained graphene/p–CdTe Schottky diodes are sharp surface-barrier structures with a uniform distribution of the impurity in the p–CdTe near-contact region; its concentration is consistent with its value in the starting material; which confirms the stability of the electrical parameters of the base material during the fabrication of the structures. The electrical junction thickness of the graphene/p–CdTe diodes was $d \approx 2.8$ µm.

Graphene/p–CdTe Schottky diodes can be promising for the manufacture of low-cost solar cells with optimal (in terms of photovoltaic conversion) CdTe band gap (E_g = 1.5 eV) and high absorption coefficient ($\alpha = 10^5$ cm^{-1}) under improved technological conditions, as well as with the decreased resistance of the base material.

References

1. S.V.Morozov, K.S.Novoselov, M.I.Katsnelson et al., *Phys.Rev.Lett.*, **100**, 016602 (2008). https://doi.org/10.1103/PhysRevLett.100.016602
2. K.S.Novoselov, A.K.Geim, S.V.Morozov et al., *Nature*, **438**, 197 (2005). doi:10.1038/nature04233
3. K.S.Novoselov, A.K.Geim, S.V.Morozov et al., *Science*, **306**, 666 (2004). http://dx.doi.org/10.1126/science.1102896
4. M.I.Katsnelson, *Materials Today*, **10**, 20 (2007). https://doi.org/10.1016/S1369-7021(06)71788-6
5. A.K.Geim, K.S.Novoselov, *Nature Materials*, **6**, 183 (2007). https://doi.org/10.1038/nmat1849
6. C.Soldano, A.Mahmood, E.Dujardin, *Carbon*, **48**, 2127 (2010). https://doi.org/10.1016/j
7. F.Bonaccorso, Z.Sun, T.Hasan, A.C.Ferrari, *Nature Photonics*, **4**, 611 (2010). http://dx.doi.org/10.1038/nphoton.2010.186
8. A.D.Bartolomeo, *Physics Reports*, **606**, 1 (2016). https://doi.org/10.1016/j.physrep.2015.10.003
9. X.Wang, L.Zhi, K.Mullen, *Nano Lett.*, **8**, 323 (2008). DOI: 10.1021/nl072838r
10. H.Bi, F.Huang, J.Liang et al., *Adv.Mater.*, **23**, 3202 (2011). DOI: 10.1002/adma.201100645
11. H.Bi, F.Huang, J.Liang et al., *J.Mater. Chem.*, **21**, 17366 (2011). DOI:10.1039/C1JM13418C
12. Z.Shi, A.H.Jayatissa, *Materials*, **11**, 36 (2018). https://doi.org/10.3390/ma11010036
13. S.Lin, X.Li, S.Zhang et al., *Appl.Phys.Lett.*, **107**, 191106 (2015). http://dx.doi.org/10.1063/1.4935426
14. J.Liang, H.Bi, D.Wan et al., *Adv.Funct. Mater.*, **22**, 1267 (2012). https://doi.org/10.1002/adfm.201102809
15. M.Aldosari, H.Sohrabpoor, N.E.Gorji, *Superlattices Microstruct.*, **92**, 242 (2016). https://doi.org/10.1016/j.spmi.2016.02.023
16. V.V.Brus, O.L.Maslyanchuk, M.M.Solovan et al., *Sci.Rep.*, **9**, 1065 (2019). https://doi.org/10.1038/s41598
17. E.Y.Polyakova(Stolyarova), K.T.Rim, D.Eom et al., *ACS Nano*, **5**, 6102 (2011). https://doi.org/10.1021/nn1009352
18. M.Yi, Z.Shen, *Carbon*, **78**, 622 (2014). https://doi.org/10.1016/j.carbon.2014.07.035
19. C.Du, S.Wang, X.Miao et al., *Beilstein J. Nanotech.*, **10**, 2374 (2019). https://doi.org/10.3762/bjnano.10.228
20. M.Mohamed, M.Tripathy, A.A.Majeed, *Arab. J.Chem.*, **10**, S1726 (2013). https://doi.org/10.1016/j.arabjc.2013.06.022
21. K.R.Zanio, Semiconductors and Semimetals. Volume 13: Cadmium Telluride. NY:SanFrancisko, Acad. Press (1978).
22. A.Niemegeers, M.Burgelman, *J.Appl.Phys.*, **81**, 2881 (1997). https://doi.org/10.1063/1.363946
23. E.V.Maistruk, I.G.Orletsky, M.I.Ilashchuk et al., *Semicond.Sci.Tech.*, **34**, 045016 (2019). https://doi.org/10.1088/1361-6641/ab0a1c
24. I.P.Koziarskyi, E.V.Maistruk, I.G.Orletskyi et al., *Semicond.Sci.Tech.*, **35**, 025018 (2020). https://doi.org/10.1088/1361-6641/ab6107
25. A.M.Goodman, *J.Appl.Phys.*, **34**, 329 (1963). https://doi.org/10.1063/1.1702608
26. I.G.Orletskyi, M.I.Ilashchuk, M.M.Solovan et al., *Mater.Res.Express*, **6**, 086219 (2019). https://doi.org/10.1088/2053-1591/ab26f3